Journal of Power Sources 182 (2008) 141–144

Contents lists available at ScienceDirect

Journal of Power Sources

journal homepage: www.elsevier.com/locate/jpowsour

Short communication

Prediction of H_2 leak rate in mica-based seals of planar solid oxide fuel cells

Shaobai Sang[a], Jian Pu[a], Sanping Jiang[b], Li Jian[a,*]

[a] College of Materials Science and Engineering, Huazhong University of Science and Technology, State Key Laboratory of Material Processing and Die & Mould Technology, 1037 Luo Yu Lu, Wuhan 430074, PR China
[b] School of Mechanical and Aerospace Engineering, Nanyang Technological University, Singapore 639798, Singapore

ARTICLE INFO

Article history:
Received 7 February 2008
Received in revised form 27 March 2008
Accepted 28 March 2008
Available online 8 April 2008

Keywords:
SOFC
Compressive seal
Mica
Leak rate

ABSTRACT

Mica-based materials, either laminated papers or layered single crystals, are popular in solid oxide fuel cell applications as sealing components. Their interface and bulk leak paths can be considered as slits with various heights, lengths and widths. A hydromechanics model was established based on the geometric assumptions to predict the influence of slit geometry and pressure difference of the seal on H_2 leak rate. The dependence of leak rate on slit geometry and the pressure difference as well as the effectiveness of compressive loading and compliant interface layer were discussed accordingly. The model's applicability is supported by reported experiments.

1. Introduction

Among the technical challenges in developing planar solid oxide fuel cells (SOFCs), the sealing material has been regarded as one of the most significant issues. The seals are required to be non-conductive, and thermally, chemically and mechanically stable in both oxidizing and reducing environments, and prevent fuel and oxidant gas leak within the stack [1–3].

The commonly used seals for the planar SOFCs have been glasses or ceramic-glasses [2]. The advantage of glass and ceramic-glass seals is that their compositions can be tailored to optimize the required physical properties, such as the coefficient of thermal expansion (CTE); however, they tend to transform in phases and react with the cell component and interconnect materials under SOFC operating conditions in a long run, due to their intrinsic thermodynamical instability [4–6].

Compressive seals have been developed to avoid the disadvantages of the rigid glass-based seals, with the merit of flexibility and compressibility; a close match of CTE to those of the adjacent materials is not required, allowing the cells and interconnects to expand and contract freely during thermal cycles and operation, and the replacement of the malfunctioning components became possible [7]. So far, two kinds of compressive seals have been considered, i.e., the deformable metallic seals and the mica-based seals. The deformable metallic seals include ductile silver [8,9] and corrugated or C-shaped superalloy gaskets [10]. Its application is limited by its high electronic conductivity [9,10]. The plain mica seals and hybrid mica-based seals have been systematically investigated and their sealing properties were reported [11–20]. The plain mica has exhibited very poor sealing characteristics, and in contrast, the hybrid mica-based seals have demonstrated excellent hermetic property and are being regarded as the potential candidate for intermediate temperature planar SOFCs. It has been identified [7,17,19] that there are two kinds of possible leak paths for mica-based seals: one is through the body of the mica (bulk leak) and the other is through the sealing interfaces between the mica and the adjacent SOFC components (interface leak). Such interfaces are considered to be the major leak paths of the conventional mica seals. The purpose of the present study is to develop a hydromechanics model to predict the leak rate; and accordingly, the factors that control the leak rate can be identified and analyzed, and appropriate sealing design procedures can be suggested to improve the hermetic property of the mica-based seals.

2. Modeling

In planar SOFCs, H_2 is usually used as the fuel, and the sealing requirement is higher than other gases due to the small molecule size of H_2. In the present study, H_2 is chosen as the subject of investigation, ideal gas assumption is applied owing to its high rarefaction.

It has been observed by a scanning electron microscope (SEM), that the leak paths of mica seals, either muscovite single crystal and paper [11] or phlogopite paper [16], are mainly composed of tiny openings located either at the sealing interfaces or in between

* Corresponding author.
E-mail address: plumarrow@126.com (L. Jian).

0378-7753/$ – see front matter © 2008 Elsevier B.V. All rights reserved.
doi:10.1016/j.jpowsour.2008.03.081

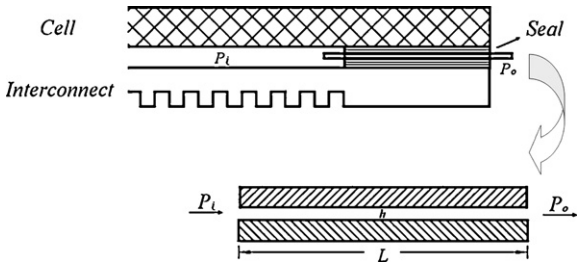

Fig. 1. Schematic illustration of sealing configuration in a planar SOFC stack.

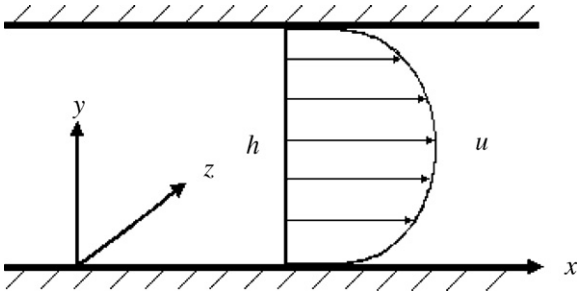

Fig. 2. Flow field set up in Cartesian coordinates.

mica layers. Both leak paths can be idealized as the slits with specific geometry, as schematically shown in Fig. 1. L is the slit length, which is more or less related to the sealing width. The slit may not be smooth, and the surface roughness is likely to be in the same order of magnitude as that of the molecular free path of H_2. H_2 leaks through the slits once the pressure inside of the stack (inner pressure) P_i is bigger than the pressure of outside of the stack (external pressure) P_o that equals to the atmospheric pressure (see Fig. 1). Since the flow is in such a confined channel, the flow characteristics of the high-temperature gas should be considered.

In hydromechanics, the non-dimensional parameter Kn, the extent of gas rarefaction, is defined as $Kn = \lambda/D$, where λ is the mean free path of gas molecules and D is the flow dimension that herein represents the slit height h. The value of Kn determines the nature of the flow. For the continuum flow, Kn is less than 0.1; the slip flow has a value of Kn in the range of 0.01–0.1; for the transition flow, Kn is in between 0.1 and ~10; and for the free-molecular flow, Kn is larger than 10.

The mean free path of gas molecules λ can be expressed as

$$\lambda = \frac{kT}{\sqrt{2}\pi d^2 P} \tag{1}$$

where k is Boltzmann constant, T is absolute temperature, d is effective diameter of gas molecular, and P is gas pressure. The average molecular free path of H_2 gas is 0.63 μm in a planar SOFC operated at 800 °C. If a slit height (h) range of 0.2–20 μm is assumed according to the observation, the pressure-driven leak flow of H_2 gas falls into the regime of the slip flow or the transition flow.

In the slip flow regime and the transition flow, the usually assumed no-slip boundary condition is no longer suitable and the Knudsen layer with a thickness of approximately a molecular free path plays a decisive role; in addition, the collisions between the gas molecule and the slit wall become more and more important compared to the collisions among gas molecules; and the kinematic viscosity needs to be modified for the enhanced rarefaction effect. Therefore a unified flow model for both the slip and transition flow regimes is to be developed, in which the flow in the slit is assumed to be divided as the Knudsen layer and the middle layer, the flow transition from the Knudsen layer to the middle layer is continuous, and the enhanced rarefaction effect is taken into account by introducing the rarefaction coefficient $C_r(Kn)$, a function of Kn.

The flow in the Knudsen layer does not follow the Navier–Stokes equation; a specific solution from the Boltzmann equation is needed. However, it is intricate to solve the Boltzmann equation, only some semi-analytic solutions or numerical solutions can be derived for special cases. Therefore, it is necessary to simplify the solving process without changing the dependence of the velocity slip boundary condition on Kn. Usually, for a relatively accurate prediction of gas flow rate (leak rate), second order precision velocity slip boundary condition is enough. So the general velocity slip boundary condition was adopted. For the pressure-driven incompressible flow in the slits, the velocity slip boundary condition [21] is

$$U_s = \frac{h^2}{2\mu}\frac{dP}{dx}\frac{Kn}{1+Kn} \tag{2}$$

where μ is the viscosity coefficient. Considering the leak flow of H_2 in a planar SOFC, further pre-conditions are given as follows:

(1) All the flows are isothermal and steady.
(2) Temperature gradient is neglected inside the leak flow of H_2.
(3) The inertia term is ignored, which is much smaller compared to the diffusion term in the momentum equations, due to the Reynolds number of the flow is low in channels with a large length/height ratio ($L/h \gg 1$).
(4) The rarefaction coefficient $C_r(Kn)$ is given as

$$C_r(Kn) = 1 + \alpha\, Kn \tag{3}$$

where $\alpha = 1.358(2/\pi)\tan^{-1}(2.2\, Kn^{0.5})$ [21].

Based on the above assumptions, the velocity distribution in the slit can be acquired, and finally the mass flow rate per flow width is derived by the integral of the flow velocity.

It is assumed that the leak flow is a steady state flow, independent of time. The streamline direction was set along the x-axis of the Cartesian coordinates as shown in Fig. 2, consequently, the flow velocity has only a component u in the x-direction; in the y and z directions, the components are zero, that is, $v = w = 0$, and the continuity equation for incompressible fluids becomes

$$\frac{\partial u}{\partial x} = 0.$$

Since u is constant in the z-direction, i.e., $\partial u/\partial z = 0$, hence, u is only a function of y, $u = u(y)$.

If the viscosity coefficient μ of H_2 is constant, Navier–Stokes equations can be written as

$$\rho\frac{du}{dt} = \rho g_x - \frac{\partial P}{\partial x} + \mu\left(\frac{\partial^2 u}{\partial x^2} + \frac{\partial^2 u}{\partial y^2} + \frac{\partial^2 u}{\partial z^2}\right) \tag{4}$$

$$\rho\frac{dv}{dt} = \rho g_y - \frac{\partial P}{\partial y} + \mu\left(\frac{\partial^2 v}{\partial x^2} + \frac{\partial^2 v}{\partial y^2} + \frac{\partial^2 v}{\partial z^2}\right) \tag{5}$$

$$\rho\frac{dw}{dt} = \rho g_z - \frac{\partial P}{\partial z} + \mu\left(\frac{\partial^2 w}{\partial x^2} + \frac{\partial^2 w}{\partial y^2} + \frac{\partial^2 w}{\partial z^2}\right) \tag{6}$$

Ignoring the gravity force of H_2, $g_x = g_y = g_z = 0$, the above equations are simplified as

$$0 = -\frac{\partial P}{\partial x} + \mu\frac{\partial^2 u}{\partial y^2} \tag{7}$$

$$0 = -\frac{\partial P}{\partial y} \tag{8}$$

$$0 = -\frac{\partial P}{\partial z} \tag{9}$$

P is only the function of x. Since the pressure difference between P_i and P_o is small, $\partial P/\partial x$ can be considered as a constant, and u can be obtained by integral of Eq. (7).

$$u = \frac{1}{2\mu}\frac{\partial P}{\partial x}y^2 + C_1 y + C_2 \tag{10}$$

Applying the boundary conditions $u(0) = u(h) = U_s$, the velocity distribution in the streamline direction is derived as

$$U(y) = \frac{h^2}{2\mu}\frac{dP}{dx}\left(\frac{y^2}{h^2} - \frac{y}{h} + \frac{Kn}{1+Kn}\right) \tag{11}$$

The volume flow rate in an unit cross-section can be obtained accordingly as

$$\dot{Q} = \int_0^h U(y)\,dy = -\frac{h^3}{12\mu}\frac{dP}{dx}\left[1 + \frac{6\,Kn}{1+Kn}\right] \tag{12}$$

Considering the effect of enhanced rarefaction and $dP/dx = -(P_i - P_o)/L$ (L is the depth of the slit), Eq. (14) is modified as

$$\dot{Q} = \frac{h^3}{12\mu}\frac{P_i - P_o}{L}\left[1 + \frac{6\,Kn}{1+Kn}\right]C_r(Kn) \tag{13}$$

And therefore, the associated mass flow rate of a single slit with a unit width can be expressed as

$$\begin{aligned}\dot{M} &= 1\rho\dot{Q} = \frac{2P_o}{RT}\frac{h^3}{12\mu}\frac{P_i - P_o}{L}\left[1 + \frac{6\,Kn}{1+Kn}\right]C_r(Kn)\\ &= \frac{P_o(P_i - P_o)h^3}{12\mu RTL}\left[(\Pi + 1) + 2(6+\alpha)Kn\right.\\ &\quad \left. + 12\frac{\alpha - 1}{\Pi - 1}Kn^2\ln\left(\frac{\Pi + Kn}{1+Kn}\right)\right]\end{aligned} \tag{14}$$

where $\rho = 2P_o/RT$ and $\prod \equiv P_i/P_o$.

In reality, there are numerous (n_i) leak paths similar to Fig. 1 in a mica-based seal with various slit height h_i and width b_i ($i = 1, 2, 3, \ldots, k-1, k$), the total leak mass flow rate is the weighted summation of $\dot{M}_i$ in terms of slit number and width.

$$\dot{M}_{total} = \sum_{i=1}^{k} n_i b_i \dot{M}_i \tag{15}$$

3. Discussions

The leak mass flow rate expressed by Eq. (14) for one slit shows that $\dot{M}$ is a function of slit height h nearly up to the third power. Fig. 3 demonstrates the dependence of H_2 leak rate at 1073 K on h with P_i as 1.048×10^5 Pa, μ as 1.92×10^{-7} Pa S, and the slit length L as 1 cm. The H_2 leak rate decreases sharply with the decreasing of h: $\dot{M}$ is 4.51×10^{-8}, 8.19×10^{-6} and 1.56×10^{-4} g s^{-1} cm^{-1} when h is 0.5, 5 and 15 μm, respectively, 30 times increase in h results in ca. 3500 times increase in leak rate. This reflects the strong impact of Knudsen flow and the associated rarefaction effect on the mass leak rate, the smaller the slit height, the more significant the influence of the Knudsen flow.

According to Eq. (14), $\dot{M}$ is proportional to $1/L$ when other parameters remain unchanged. The slit length is somewhat related to the sealing width. If a single slit penetrates the entire sealing width, L is equal to the sealing width; however, in a real mica-based seal, a single leak slit usually can only penetrate a portion of the sealing width, the actual leak path is proportional to, but much longer than the sealing width, and the leak rate will be dramatically decreased by increasing the sealing width. In a specific stack design, increasing sealing width may cost the active area and power output, therefore, the effectiveness of lowering the leak rate by increasing leak path L is limited in real applications.

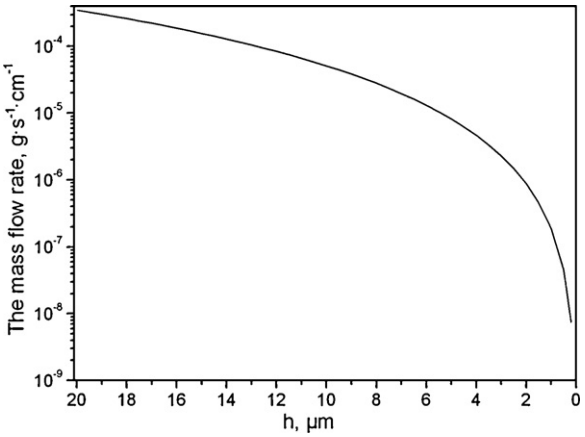

Fig. 3. Model prediction of H_2 mass leak rate as a function of slit height.

For a specific leak slit with a width of b_i, the contribution of the slit width to the mass leak rate is demonstrated in Eq. (15) as a factor of the unit width leak rate $\dot{M}$. From Eq. (15), it also can be seen that the total mass leak rate is proportional to the leak slit size distribution ($n_1, n_2, n_3, \ldots, n_i, \ldots, n_k$) and the total leak slit number N ($N = \sum_1^k n_i$). With the same total slit number N, the total mass leak rate may be different, depending on the distribution (n_1, n_2, $n_3, \ldots, n_i, \ldots, n_k$). On the other hand, a smaller N may result in a bigger leak rate than a bigger N, if the slit size distribution (n_1, n_2, $n_3, \ldots, n_i, \ldots, n_k$) represents more large leak slits, especially with bigger h.

In order to drive the gas flow, the gas pressure inside the SOFC stacks is usually 1.4–3.5 kPa (0.2–0.5 psi) higher than the outside atmosphere pressure, and may be increased to 1.4×10^4 Pa (2 psi) with the fluctuation of source gas pressure. Fig. 4 shows the H_2 leak rate with different P_i and constant h (1 μm) and L (1 cm). The H_2 mass leak rate decreases linearly with ($P_i - P_o$), which is consistent with the previous study [11] where the leak rates of phlogopite paper, muscovite paper and muscovite single crystal were measured against the gauge pressure.

Based on the analysis above, two suggestions can be made for a tighter sealing: (1) increasing the compressive load; and (2) applying a compliant layer, such as soft metal or glass, at the sealing surfaces. With higher compressive stress, the slit height

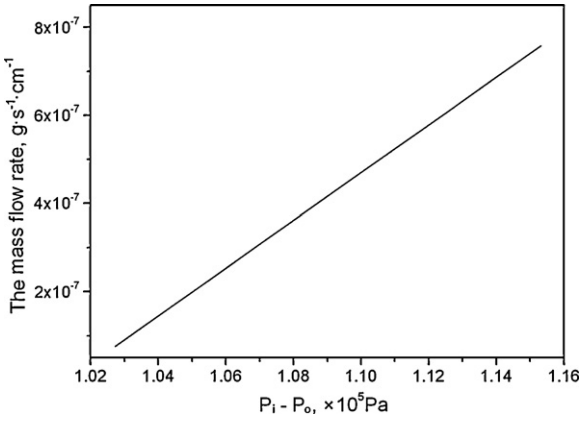

Fig. 4. Model prediction of H_2 mass leak rate as a function of pressure difference between inside and outside of SOFC stack.

h and width b tends to be smaller and some tiny leak slits may be completely closed, resulting in a lower leak rate. Jeffrey's work [2] showed that the leak rate for all kinds of the mica seals, no matter mica papers or single crystal layers, decreased with increasing applied compressive stress, which is supportive to the model prediction. For muscovite single crystals, increasing compressive loading is more effective due to its smoother slit surfaces and readiness for slit closure; a leak rate of 1/10 to ~1/5 of that from the mica papers was achieved at the same compressive pressure [11]. The robustness of mica-based sealing can be further improved by using a silver or specific glass at the sealing surface, which can eliminate the major leak paths in the interface; or by infiltration of a second phase, such as glass, to seal the interface and bulk leaks, a leak rate down to 1.3×10^{-4} sccm cm^{-1} can be resulted [17].

4. Conclusions

According to the model study and experiment comparison, the following conclusions can be made:

(1) The leak paths in mica-based seals can be simulated as slits with various heights h, lengths L and widths b. The leak rate is a function of the slit height h *nearly up to the third power*, and is proportional to the slit width and the reciprocal of the slit length.
(2) The total leak rate increases with the total slit number of the seal N, and is strongly related to the slit size distribution (n_1, n_2, n_3, . . ., n_i, . . ., n_k).
(3) Pressure difference between inside and outside of the cell drives H_2 leaking through the seal, and the leak rate is proportional to the pressure difference.
(4) Increasing the compressive loading and applying compliant interlayer improve the robustness of the seal by reducing the leak slit size and seal the leak paths at the sealing interfaces.

Acknowledgements

This project is financially supported by National "863" program of China under the contract 2006AA05Z148 and Wuhan Science and Technology Bureau for key project 200710321087.

References

[1] R.N. Singh, Ceram. Eng. Sci. Proc. 25 (3) (2004) 299–307.
[2] W.F. Jeffrey, J. Power Sources 147 (2005) 46–57.
[3] C.A. Lewinsohn, S. Elangovan, S.M. Quist, Ceram. Eng. Sci. Proc. 25 (3) (2004) 315–320.
[4] L. Peng, Q.S. Zhu, C.H. Xie, et al., J. Inorg. Mater. (Chin.) 21 (4) (2006) 867–872.
[5] S.P. Jiang, L. Christiansen, B. Hughan, K. Foger, J. Mater. Sci. Lett. 20 (8) (2001) 695–697.
[6] Z. Yang, J.W. Stevenson, K.D. Meinhardt, Solid State Ionics 160 (2003) 213–225.
[7] L. Shiru, S. Kening, N. Zhang, et al., J. Power Sources 161 (2006) 901–906.
[8] J. Duquette, A. Petric, J. Power Sources 137 (1) (2004) 71–75.
[9] Y.S. Chou, J.W. Stevenson, J. Mater. Res. 18 (9) (2003) 2243–2250.
[10] M. Bram, S. Rechers, P. Drinovac, et al., J. Power Sources 138 (1–2) (2004) 111–119.
[11] S.P. Simner, J.W. Stevenson, J. Power Sources 102 (1–2) (2001) 310–316.
[12] Y.S. Chou, J.W. Stevenson, L.A. Chick, J. Power Sources 112 (1) (2002) 130–136.
[13] Y.S. Chou, J.W. Stevenson, J. Power Sources 112 (2) (2002) 376–383.
[14] Y.S. Chou, J.W. Stevenson, J. Power Sources 115 (2) (2003) 274–278.
[15] Y.S. Chou, J.W. Stevenson, L.A. Chick, J. Am. Ceram. Soc. 86 (6) (2003) 1003–1007.
[16] Y.S. Chou, J.W. Stevenson, J. Power Sources 124 (2) (2003) 473–478.
[17] Y.S. Chou, J.W. Stevenson, J. Power Sources 135 (1–2) (2004) 72–78.
[18] Y.S. Chou, J.W. Stevenson, J. Power Sources 140 (2) (2005) 340–345.
[19] Y.S. Chou, J.W. Stevenson, P. Singh, J. Power Sources 152 (2005) 168–174.
[20] Y.S. Chou, J.W. Stevenson, P. Singh, J. Power Sources 157 (2006) 260–270.
[21] G.E. Karniadakis, A. Beskok (Eds.), Micro Flow Fundamentals and Simulation, Springer-Verlag, New York, 2002.